

Lateral flow in loamy to sandy Kandiuults of the Upper Coastal Plain of Georgia (USA)

J.N. Shaw ^{a,*}, D.D. Bosch ^b, L.T. West ^c, C.C. Truman ^b,
D.E. Radcliffe ^c

^a Auburn University, Department of Agronomy and Soils, 202 Funchess Hall, Auburn,
AL 36849-5412, USA

^b USDA-SE Research Watershed Laboratory, P.O. Box 946, Tifton,
GA, 31794, USA

^c University of Georgia, Department of Crop and Soils, 3111 Miller Plant Sci. Bldg., Athens,
GA 30602, USA

Received 12 May 1999; received in revised form 27 April 2000; accepted 1 May 2000

Abstract

Interest in site-specific agronomic management in intensively cropped regions necessitates characterization of subsurface water movement for efficient water management (irrigation timing) and control of off-site agrichemical movement. Soils formed in fluvial sediments in portions of the Upper Coastal Plain of Georgia (USA) are extensively used for peanut, cotton, and corn production. Certain proximate soils in this region possess contrasting subsoil properties, and it was hypothesized that these differences would have major effects on water redistribution across the landscape. This could be important in irrigation management, where soils possessing increased impedance to vertical flow could require decreased irrigation as opposed to soils without vertical flow restrictions. At a site near Plains, GA. (USA), hydraulic properties of soils with differences in overlying sand thickness and contrasting argillic horizon textures (sandy vs. loamy) were evaluated. The soils were predominantly in loamy and sandy families of Typic, Arenic, and Grossarenic Kandiuults. Laboratory measurements, field monitoring of matric potentials under simulated and natural rainfall, and modeling (VS2DT) were utilized to evaluate soil hydraulic properties. Reduction in vertical K_s occurred in horizons containing higher clay (argillic horizon). Changes in tension and build ups in hydraulic gradients associated with infiltration and redistribution events existed above and within horizons with low K_s . Evidence suggested there was less groundwater recharge occurring in the loamy than in the sandy pedons, suggesting more

* Corresponding author. Tel.: +1-334-844-3957; fax: +1-334-844-3945.
E-mail address: jnshaw@acesag.auburn.edu (J.N. Shaw).

pronounced lateral flow occurred in the loamier soils. Model simulations of water movement across a slightly sloping (1%) simulated landscape indicated lateral gradients of flow existed within the solum of these soils. Analyses of tracer (Br) movement suggested a very slight lateral redistribution occurred within a relatively short monitoring period within the sandy pedon's Bt1 horizon, and the Bt2 and Bt3 horizons of the loamy pedon. Evidence suggested both loamy and sandy argillic horizons slightly, but not overwhelmingly, induced lateral flow on these landscapes. © 2001 Elsevier Science B.V. All rights reserved.

Keywords: vadose zone; coastal plains; hydraulic conductivity; lateral flow

1. Introduction

Pedogenic (clay translocation) and depositional processes create soil horizons that can affect transient water movement in the vadose zone (Bruce and Whisler, 1973; Wilson et al., 1990; Shaw et al., 1997). Particle-size differences create soil interfaces that can act as impermeable lenses, e.g., soil horizons containing abundant clay inhibit vertical movement of water as infiltration is typically faster than percolation through the argillic horizon (Kung, 1990a; Jury et al., 1991). If sufficient restriction occurs, lateral flow can be induced above and within these less permeable zones. Lateral flow can result in elevated pollution of surface and groundwater where decreased transport times do not allow for the renovation effects of soils (Chappall et al., 1990). In addition, differences in subsoil permeability can affect irrigation timing.

Hydrologists have investigated the effects of shallow subsurface features on lateral water movement in the vadose zone, with emphasis on streamflow evolution and water quality (Anderson and Burt, 1990; McDonnell, 1990; Wilson et al., 1991, 1993; Ross et al., 1994; Nyberg, 1995). A significant lateral flow component on a hillslope is often associated with layers with reduced permeability relative to the overlying horizons (Gaskin et al., 1989; Wilson et al., 1990; Bosch et al., 1994). Shallow subsurface water-restrictive features are often pedogenic in origin; e.g., argillic horizons, and positive pressure potentials have been shown to occur above argillic horizons during infiltration events (Bruce and Whisler, 1973). Wilson et al. (1990) found perched water tables above argillic horizons in Ultisols in Tennessee (USA). They concluded that during storm events, macropore flow through overlying eluvial horizons resulted in near saturated conditions above the argillic horizon leading to downslope water movement along its upper portion. In landscapes containing variation in argillic horizon expression, the occurrence and degree of water perching can be quite different. Coarse sands can also induce hydraulic barriers and lateral flow under unsaturated conditions. Even when steep pressure head gradients exist across a fine and coarse textured interface, air-filled pores and the small effective cross-section prevent flow into coarse material (Jury et al., 1991). Kung (1990b) studied the effects of sandy layers on water movement in a

Plainfield loamy sand (USA) (sandy, mixed, mesic Typic Udipsamment) where coarse sand lenses were interbedded with fine sands. Dye patterns indicated that water moved laterally over coarse sand wedges after vertically infiltrating into finer sand lenses. Coarse sand lenses, if sloped, can act to funnel the water flow and create irregularly spaced columns of water movement.

In our region (southwest Georgia, USA), many upland soils possess coarse-textured epipedons with high infiltration rates, and subsurface horizons of reduced K_s . The presence and permeability of these underlying horizons greatly influences soil hydraulic properties (Blume et al., 1987). Most soils of the region have an appreciable clay increase in the solum, but soils with loamy sand and sandy loam (5 to 20% clay) textured argillic horizons are common (sandy and coarser textured loamy families of Grossarenic Kandiodults) (Pilkinton, 1974; Shaw et al., 2000). These soils with sandy argillic horizons are geomorphically associated with soils that possess better developed argillic horizons (20% to 40% clay) and are correspondingly classified in loamy and fine-loamy families of Typic, Arenic, and Grossarenic Kandiodults (Hicks et al., 1991a; Bosch and West, 1998).

Because of the intensive row-crop agriculture, studies on agrichemical movement into groundwater have been conducted in this region. Groundwater/agrchemical fate investigations in this region at a site near Plains, GA., have shown atrazine and its metabolite, desethylatrazine (DEA), were at maximum concentrations in groundwater 60 m down gradient from the application point, with smaller amounts being detected 280 m down gradient (Leonard et al., 1993). At the same site but shallower in the profile, Hicks et al. (1991b) investigated movement of a Br tracer and hypothesized an appreciable amount of lateral transport in the vadose zone occurred that was possibly due to local regions of decreased K_s . In similar soils, Bosch and West (1998) have shown that subsoil K_s decreased with increasing clay content as soils graded from sandy (5% to 15% clay) to loamy (30% to 35% clay) argillic horizons.

It is hypothesized on these landscapes that water distribution in the vadose zone is controlled largely by argillic horizons of variable conductivity. In other landscapes of the region, Bosch et al. (1994) have shown that significant vertical flow impedance and lateral flow is induced by well defined argillic horizons containing plinthite. However, due to the range in argillic horizon characteristics of the studied associated soils, the degree of vertical flow inhibition and possible lateral flow is hypothesized to vary. Besides ramifications for groundwater contamination potential, soils with contrasting hydraulic properties in the solum affect irrigation timing, i.e., soils that inhibit vertical water movement may require less frequent irrigations than highly permeable soils that require more frequent, less intense irrigation. Thus, our objectives were to: (1) evaluate hydraulic properties of these predominantly sandy soils with contrasting subsoil textures, and (2) evaluate if argillic horizons act as impeding layers that may induce lateral flow.

2. Materials and methods

Sumter county, located in southwestern Georgia, lies within the Coastal Plain physiographic province. Deep geologic materials in this area were derived from fluvio-marine deposited gravel, sand, silt and clay. The research site, near Plains (Sumter), GA (Fig. 1) ($31^{\circ}59'0''$ to $45''$ N; $84^{\circ}24'0''$ to $30''$ W), is located in the southern portion of the Fall Line Hills region, and is underlain by: (1) the (> 12 m below the surface) Tuscaloosa formation (Paleocene age); and (2) the shallower Tallahatta formation (≈ 3 to 12 m) (Eocene age) (Hicks et al., 1991b; Stewart and Hicks, 1996). The Claiborne aquifer is contained dominantly in the lower Tallahatta formation and is relatively unconfined and generally reflective of surface topography (Hicks et al., 1991b). Since sediment deposition, fluvial events and dissection of terraces have altered the landscapes. The research site is situated on an interfluvial/fluvial terrace landscape position, and soils have mostly developed in fluvial parent materials (Fig. 1). The west portion of the site is bounded by the third order Ty Ty creek, and the east side is bordered by a first order tributary. The uplands range in elevation from 125 to 145 m, and the surface slopes to the south (1%) at the crest.

Two 10×10 m² subplots (NW and SE) were established on this interfluvial in areas that have soils with the extremes of argillic horizon clay content and sandy

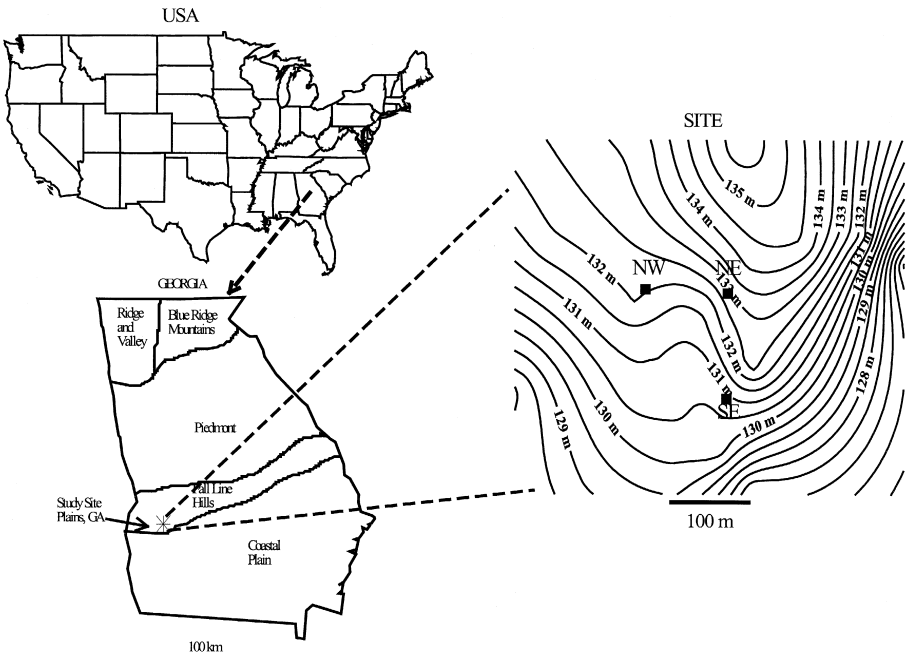


Fig. 1. Location of site near Plains, GA (USA), and the location of the subplots.

epipedon thickness found in upland positions of this region. Adjacent to each subplot, pits were excavated, and pedons were described, sampled, and classified according to standard Soil Survey Staff (1996) techniques. An additional pedon was sampled in the NE corner, but no subplot was established as this soil possessed properties intermediate of the NW and SE pedons. Soils examined classified into coarse-loamy, kaolinitic, thermic Typic Kandiuults in the SE; loamy, kaolinitic, thermic Grossarenic Kandiuults in the NW; and loamy, kaolinitic, thermic Grossarenic Kandiuults in the NE. The SE soil possessed the most clayey argillic horizon, the NW soil had the sandiest, and the NE was intermediate (Table 1). Saturated hydraulic conductivity (K_s) measurements

Table 1
 K_s data and selected physical properties for pedons

Hor	Depth (cm)		K_s			
			Field mean (cm h^{-1})*	Lab horizontal (cm h^{-1})	Clay %	Bulk density (g cm^{-3})
<i>SE: coarse-loamy, kaolinitic, thermic Typic Kandiuult</i>						
Ap	0	21	11.5 (0.5) ^d	14.8	2.7	1.71
Bt1	21	52	17.1 (5.6) ^d	19.9	11.6	1.67
Bt2	52	92	12.1 (2.7) ^d	19.9	13.2	1.61
Bt3	92	126	11.2 (9.5) ^d	31.0	16.3	1.65
Bt4	126	164	3.3 (3.3) ^d	5.6	28.1	1.69
Bt5	164	250	6.3 (11.4) ^d	5.2	27.1	1.73
BC1	250	293	3.0 (2.3) ^d	–	27.9	–
BC2	293	340	42.2 (56.6) ^{c,d}	–	21.5	–
BC3	340	393	28.4 (31.5) ^{c,d}	–	14.7	–
CB1	393	445	431.0 (19.2) ^a	–	2.2	–
<i>NW: loamy, kaolinitic, thermic Grossarenic Kandiuult</i>						
Ap	0	26	30.2 (17.0) ^{c,d}	23.0	3.4	1.77
E1	26	75	52.4 (33.3) ^{b,c,d}	–	4.1	1.70
E2	75	109	77.7 (5.2) ^{b,c}	33.1	4.4	1.62
E3	109	138	108.4 (85.4) ^b	–	5.8	1.65
Bt1	138	191	14.4 (6.9) ^d	22.1	15.2	1.70
Bt2	191	246	32.0 (1.2) ^{c,d}	–	14.1	–
BC	246	300	31.9 (0.4) ^{c,d}	25.1	9.7	–
CB	300	366	39.7 (12.1) ^{c,d}	–	7.8	–
C1	366	434	48.6 (37.2) ^{c,d}	–	6.4	–
<i>NE: loamy, kaolinitic, thermic Grossarenic Kandiuult</i>						
Ap	0	26	16.4 (1.3) ^d	20.9	3.7	1.69
E	26	110	45.3 (48.7) ^{c,d}	27.3	9.0	1.63
Bt	110	200	12.7 (1.6) ^d	10.5	21.0	1.71

* Numbers in parentheses are standard deviations. Means with superscripts of the same letter are not significantly different at the $p = 0.05$ level.

were conducted within each horizon in the field using the Compact Constant Head Permeameter (CCHP) borehole technique (Amoozegar, 1989).

2.1. Laboratory

Bulk samples collected as above were air-dried and weighed, and coarse fragments were removed by crushing samples and dry sieving through a 2-mm sieve. Particle size analyses (PSA) was conducted with the pipette method (Kilmer and Alexander, 1949). Bulk density was measured by the clod method (Blake and Hartge, 1986). Horizontal and vertically oriented small cores ($8.5 \times 6 \text{ cm}^2$) were collected from each horizon for measurement of hydraulic properties. Saturated hydraulic conductivities (K_s) on small horizontal cores were measured with the constant head method (Klute and Dirksen, 1986). Water release curve measurements were conducted on vertical cores over pressures (h) from 10 to 15 000 cm H_2O . Water release data were fit to a modified van Genuchten expression (van Genuchten, 1980; Lappala et al., 1993) for comparison and for simulation model input (using the Variably Saturated Two-Dimensional Solute Transport, VS2DT; Lappala et al., 1993):

$$\theta = \left[\left[1 + (-\alpha(h))^N \right]^{\frac{1}{N}-1} \right] (\theta_s - \theta_r) + \theta_r \quad (1)$$

where: α = scaling length parameter related to the air entry potential; reciprocal of α is an estimate of the suction where the first pores empty (cm^{-1}). N = pore size distribution parameter. θ_r = residual volumetric water content ($\text{cm}^3 \text{ cm}^{-3}$). θ_s = saturated volumetric water content ($\text{cm}^3 \text{ cm}^{-3}$). h = matric potential (cm H_2O).

Curve fitting was conducted using a least squares algorithm (Marquardt–Levenburg) which minimized sums of squares. Although θ_s is sometimes fixed in this equation as equal to porosity (φ), φ was utilized only as an upper constraint since entrapped air often causes θ_s to be slightly lower than φ . Using these parameters, unsaturated hydraulic conductivity [$K(h)$] curves were developed (van Genuchten, 1980):

$$K(h) = K_s \left[1 + \alpha(-h)^N \right]^{\frac{-M}{2}} \left[1 - \left[1 - \left[1 + \alpha(-h)^N \right]^{-1} \right]^M \right]^2 \quad (2)$$

where $M = 1 - 1/N$, and K_s = saturated hydraulic conductivity (cm h^{-1}).

2.2. Field methods

During a 2-year period, tensiometers installed at 60, 90, 120, 160, 200 and 350 cm monitored soil matric potentials (h) at 1-h intervals in NW and SE

subplots. Measurements were collected utilizing calibrated pressure transducers attached to tensiometers and connected to a Campbell[®] CR 10 data logger with a multiplexer. Triplicate tensiometers were installed in each subplot at each depth (2 m apart). Some of these data exhibited a diurnal fluctuation as displayed by rapidly ascending and descending data, most likely associated with the heating and cooling of the column above the water in the tensiometers (Cassel and Klute, 1986; Butters and Cardon, 1998). This was differentiated from changes in moisture status.

2.3. Rainfall simulations

Two simulated rainfall events were applied to portions ($10 \times 5 \text{ m}^2$) of each of the subplots. Subplot surfaces were roto-tilled prior to applying rainfall, and strips of furnace filter were placed on the surface to minimize surface crusting and maintain infiltration. The first simulation was conducted in January, 1995. Experiments were conducted by raining (water obtained from adjacent well) for 1 h, taking measurements, then raining for an additional hour. Rainfall intensities were 4.74 (1st hour) and 4.46 (2nd hour) cm h^{-1} for the NW subplot, and 4.25 (1st hour) and 3.86 (2nd hour) cm h^{-1} for the SE subplot. During rainfall events, h was monitored in both plots with tensiometers nests as described above (logged at 5-min intervals). Soil moisture was monitored (15 cm depth increments) at select times with a Troxler[®] Capacitance Probe.

During the second simulation (August, 1995), rainfall intensities were 4.64 (1st hour), and 4.82 (2nd hour) cm h^{-1} for the NW site, and 3.08 (1st hour), and 4.03 (2nd hour) cm h^{-1} for the SE site. At each site, the simulation was conducted for 1 h, halted for 0.5 h during sample collection, then resumed for 1 h. Soil matric potential heads were monitored as above.

During the August simulation, 5 kg of KBr were placed at a 5 cm depth (approximately 30 cm in diameter) at one end of each plot under the simulators. KBr was chosen due to it is high water solubility ($53.5 \text{ g } 100 \text{ ml}^{-1}$) and relatively conservative behavior. At 1, 3, 6, 11, 17 and 45 h, soil samples were collected. Samples were taken from the center, and at 40, 65 and 90 cm from the center in four directions (N, S, E, W), at depths of 15, 30, 60, 90, and 120 cm for early sample times, with additional depths of 160 and 200 cm for later sample times. Soils were air dried, crushed, and 10 g of soil were added to 30 ml of water, and shaken for 0.5 h. Suspensions were analyzed for Br with an ion specific electrode (ISE) using a 5 M NaNO_3 (1% v/v) ionic strength adjustor with a double junction reference electrode. Due to ISE detection limits and

¹ Use of a commercial product does not indicate endorsement by the authors or their agencies.

background levels, only concentrations above 0.2 mg kg^{-1} ($1 \times 10^{-5} \text{ M}$ for 10.0 g in 30 ml) were considered. Bromide data was compiled as a function of x , y , and z coordinates.

2.4. Modeling procedure

In order to assess the probability of lateral flow and to permit a more holistic view, we used VS2DT to simulate landscape water flow (Lappala et al., 1993). VS2DT is a finite-difference model that uses numerical techniques with a fully implicit scheme to simulate two-dimensional water flow at subsequent time steps. Measured (anisotropy, K_s , α , N , θ_r , θ_s) and estimated (specific storage) hydraulic parameters for E1 and E2 horizons and Bt1 and Bt2 horizons were combined for the NW soils. Parameters for Bt2 and Bt3 horizons and Bt4 and Bt5 horizons were combined for the SE soils.

VS2DT was utilized to simulate total head (H) in a landscape cross-section (50 m length set at 1% slope to mimic the actual landscape of the site) consisting of equal proportions of the NW, NE, and the SE soil, similar to soil distribution relationships at our site. NE pedon properties were placed between the other two soil types for it possessed properties (morphological and hydraulic) intermediate of the NW and SE soils, which is typical on these landscapes (Bosch and West, 1998). The upper boundary conditions were set at a constant infiltration rate (40 mm h^{-1}) for the first recharge period (2 h), then changed to a no flow boundary (remaining 70 h). Left, right, and bottom boundaries were set to $h = -100 \text{ cm H}_2\text{O}$ during the first recharge period, then changed to $-50 \text{ cm H}_2\text{O}$ during the rest of the simulation. The distance between 10 and 40 m was evaluated on the transect to minimize any edge effects caused by the boundary conditions. Initial condition was set to a constant matric potential head ($h = -75 \text{ cm H}_2\text{O}$). The simulation was conducted for 72 h .

3. Results and discussion

3.1. Saturated hydraulic conductivity

Pedons were classified as Typic, Grossarenic, and Grossarenic Kandiodults for SE, NE, and NW subplots, respectively (Shaw et al., 2000). In the SE pedon, clay increased immediately below the surface horizon from 2.7% in the Ap to 11.6% in the Bt1, with another increase in clay from 16.3% in the Bt3 to 28.1% in the Bt4 occurring at 1.26 m (Table 1). Field K_s increased below the SE surface (Ap) horizon, from $11.5 \pm 0.5 \text{ cm h}^{-1}$ in the Ap horizon to $17.1 \pm 5.6 \text{ cm h}^{-1}$ in the underlying Bt1 horizon. A similar trend was seen in the NE

pedon, where clay increased from 3.7 to 9.0% from the Ap to the E horizon, and the K_s increased from 16.4 ± 1.3 (Ap) to 45.3 ± 48.7 (E) cm h^{-1} . Although not described, the occurrence of a traffic or plow pan at the base of the Ap horizon in these two pedons may account for the lower K_s observed in these surface horizons. A decrease in K_s from 11.2 ± 9.5 cm h^{-1} in the Bt3 to 3.3 ± 3.3 cm h^{-1} in the Bt4 occurred concurrent to the second increase in clay in the SE pedon. However, these differences in the SE pedon were not significant ($p = 0.05$). A decrease in K_s was also observed where clay increased in the NE pedon; from 45.3 ± 48.7 cm h^{-1} to 12.7 ± 1.6 cm h^{-1} in the E and Bt1 horizons, respectively. For the NW pedon, the argillic horizon began at 1.38 m (clay increased from 5.8% in the E3 to 15.2% in the Bt1), and similar to the other pedons, there was a decrease in K_s (108.4 ± 85.4 in E3 to 14.4 ± 6.9 cm h^{-1} in Bt1) associated with the increase in clay. There were significant differences ($p = 0.05$) between eluvial and illuvial horizons in this pedon (Table 1). The lowest field K_s in the SE pedon was 3.3 ± 3.3 cm h^{-1} in the Bt4 horizon, and 3.0 ± 2.3 cm h^{-1} in the BC1 horizon. These were an order of magnitude less than the lowest K_s in the NW pedon (14.4 ± 6.9 cm h^{-1} in Bt1) or the NE pedon (12.7 ± 1.6 cm h^{-1} in Bt2).

Because of the lower K_s of the argillic horizon of the SE soil, it was hypothesized the SE pedon would possibly show a higher degree of lateral flow associated with the argillic horizon than the NW pedon. Effective saturated conductivity (K_{eff}), or the depth weighted mean of the conductivity for the entire solum (through the CB horizon) of SE and NW pedons indicated the NW pedon was almost five times as conductive as the SE pedon; 35.2 cm h^{-1} for the NW pedon, to 7.5 cm h^{-1} for the SE pedon.

3.2. Water release curves

The van Genuchten (1980) expression was fit to the water release curves and parameters were averaged for each horizon (Table 2). Relatively sandier horizons (E's, Ap from NW; Bt1 from SE; Ap and E from NE) had higher N values than horizons with more clay, indicative of steeper retention curves associated with a quicker water release, and suggesting a relatively homogeneous pore system. The SE Ap horizon, although sandy, had a lower N value (1.745). Reasons for this horizon displaying water release curve characteristics of a loamier horizon were unclear, although it is probable these horizons had greater organic matter content and were slightly more compacted. Sand content was positively correlated ($r = 0.82$) with N for all horizons (Fig. 2a). Similarly, N was correlated ($r = 0.80$) with K_s (Fig. 2b). Soil descriptions indicated that sandier horizons (E's and upper Bt's) were structureless or had weak grades of structure (Shaw et al., 2000). Thus, it appeared that particle size as opposed to soil structure was having a predominant effect on moisture retention and K_s of these sandy soils.

Table 2

Moisture release curve parameters derived from van Genuchten (1980) expression

Hor	<i>n</i>	θ_s (cm ³ cm ⁻³)	θ_r (cm ³ cm ⁻³)	α (cm ⁻¹) ^a	<i>N</i>
<i>SE</i>					
Ap	4	0.32	0.05	0.039 (0.01)	1.745 (0.13)
Bt1	3	0.37	0.08	0.046 (0.01)	2.032 (0.10)
Bt2	3	0.30	0.04	0.052 (0.02)	1.603 (0.36)
Bt3	3	0.37	0.08	0.042 (0.01)	1.942 (0.04)
Bt4	5	0.32	0.09	0.026 (0.01)	1.447 (0.22)
Bt5	5	0.32	0.11	0.040 (0.02)	1.609 (0.18)
<i>NW</i>					
Ap	4	0.32	0.06	0.031 (0.01)	2.436 (0.68)
E1 and 2	8	0.33	0.07	0.046 (0.02)	2.884 (1.31)
E3	2	0.30	0.08	0.043 (0.03)	2.460 (1.43)
Bt1	4	0.35	0.09	0.056 (0.02)	1.819 (0.12)
Bt2	2	0.35	0.08	0.058 (0.02)	1.719 (0.01)
BC	3	0.34	0.07	0.074 (0.03)	2.495 (0.60)
<i>NE</i>					
Ap	3	0.34	0.07	0.035 (0.00)	2.319 (0.08)
E	2	0.36	0.07	0.038 (0.01)	2.327 (1.11)
Bt1	3	0.33	0.10	0.039 (0.01)	1.560 (0.07)

^aNumbers in parentheses are standard deviations.

3.3. Matric potentials

Monitoring of matric potentials (*h*) during natural and rainfall simulation events in the NW and SE pedons was utilized to evaluate if pedogenic horizons acted as impeding layers. There was not sufficient flow restriction to cause saturation (as determined from $h = 0$) above any horizon, or a “perched” water table in the profile under normal events. This was not surprising considering the relatively high permeability of the soils.

To evaluate differences in *h* with depth, 11 rainfall events (nine natural and two during rainfall simulation events) in the NW subplot and 10 events in the SE subplot (eight natural and two during rainfall simulation events) were analyzed (Tables 3 and 4). In general, during infiltration events retardation and redistribution of wetting fronts occurs due to differences in hydraulic conductivity, water retention, and evapotranspiration occurring with depth (Katul et al., 1997). Because of this, increases in water content became proportionally lower with depth. During the rainfall simulation events and under most of the natural events, subplots had bare (excepting furnace filter in rainfall simulation events), and many times, freshly tilled surfaces. Thus, it was hypothesized that wetting

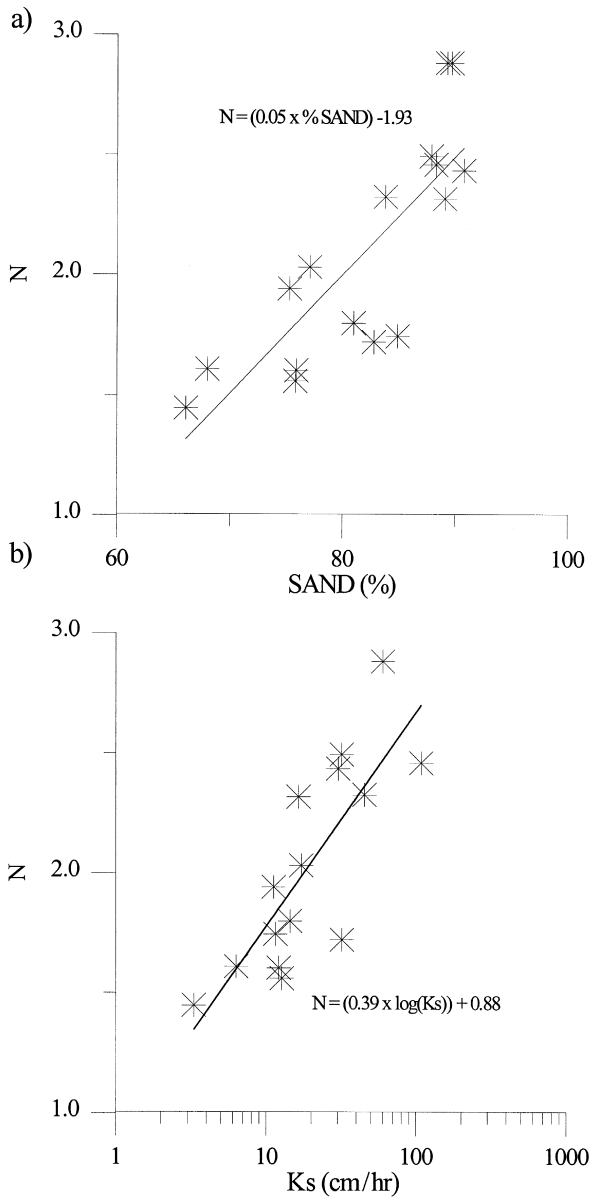


Fig. 2. (a) N vs. % sand (0.05 to 2 mm). (b) N vs. K_s .

front retardation would mainly be due to hydraulic conductivity and water retention differences and the resulting effects. The sandy epipedons possessed low water holding capacities, thus moisture retention effects as manifested by decreases in the amount of water allowed to percolate would not be as

Table 3

Difference in max. and min. matric potential heads (h) occurring within each event (NW)

NW site	Rainfall (mm)	60 (cm)	90 (cm)	120 (cm)	160 (cm)	200 (cm)	350 (cm)
<i>0602</i> (date)	74.2						
diff		70.2	53.6	55.5	74.6	73.9	40.6
rank		3.0	5.0	4.0	1.0	2.0	6.0
<i>0608</i>	105.7						
diff		30.4	56.9	63.6	59.5	15.2	21.7
rank		4.0	3.0	1.0	2.0	6.0	5.0
<i>0630</i>	69.3						
diff		20.4	20.6	15.7	20.9	12.6	16.9
rank		3.0	2.0	5.0	1.0	6.0	4.0
<i>0712</i>	101.6						
diff		38.5	24.2	24.8	30.2	23.1	12.8
rank		1.0	4.0	3.0	2.0	5.0	6.0
<i>0824</i>	170.7						
diff		32.4	58.1	49.1	71.9	39.7	15.0
rank		5.0	2.0	3.0	1.0	4.0	6.0
<i>1007</i>	70.1						
diff		40.1	30.4	31.0	36.7	30.8	16.5
rank		1.0	5.0	3.0	2.0	4.0	6.0
<i>1031</i>	41.9						
diff		na	na	na	na	na	na
rank							
<i>1201</i>	37.3						
diff		58.5	40.1	39.6	47.6	32.3	25.6
rank		1.0	3.0	4.0	2.0	5.0	6.0
<i>1201a</i>	44.2						
diff		31.9	24.1	21.6	22.2	24.8	4.7
rank		1.0	3.0	5.0	4.0	2.0	6.0
<i>jansim</i>	92.0						
diff		36.0	26.8	22.7	25.3	15.6	18.8
rank		1.0	2.0	4.0	3.0	6.0	5.0
<i>augsim</i>	94.6						
diff		120.1	47.5	42.3	51.6	30.4	37.5
rank		1.0	3.0	4.0	2.0	6.0	5.0
Avg change		43.49	34.75	33.25	40.02	27.10	19.09
Avg rank		1.91	2.91	3.27	1.82	4.18	5.00
θ_v change ^a		0.091	0.054	0.056	0.033	0.031	na ^b

^a θ_v change estimated from moisture release curve data for corresponding avg. h change.

^bNo moisture release curve data was measured at this depth to convert h to θ_v .

pronounced as in a loamier soil. However, due to the low tensions exhibited, the full ranges in differences in water holding capacities were probably not evident.

Generally, wetting fronts advanced at similar rates down to 120 cm in both soils (Figs. 3 and 4). For example, in the NW pedon during the January

Table 4

Difference in max. and min. matric potential heads (h) occurring within each event (SE)

SE site	Rainfall (mm)	60 (cm)	90 (cm)	120 (cm)	160 (cm)	200 (cm)	350 (cm)
<i>0602</i> (date)	74.2						
diff		164.0	157.7	143.6	112.5	108.1	22.2
rank		1.0	2.0	3.0	4.0	5.0	6.0
<i>0608</i>	105.7						
diff		32.5	49.1	97.9	78.5	46.2	9.0
rank		5.0	3.0	1.0	2.0	4.0	6.0
<i>0630</i>	69.3						
diff		28.9	37.2	37.1	27.0	18.9	5.5
rank		3.0	1.0	2.0	4.0	5.0	6.0
<i>0712</i>	101.6						
diff		58.4	67.4	72.8	55.7	38.5	5.7
rank		3.0	2.0	1.0	4.0	5.0	6.0
<i>0824</i>	170.7						
diff		62.8	82.7	115.8	80.0	58.9	15.0
rank		4.0	2.0	1.0	3.0	5.0	6.0
<i>1007</i>	70.1						
diff		71.4	73.7	73.8	56.0	39.5	13.0
rank		3.0	2.0	1.0	4.0	5.0	6.0
<i>1031</i>	41.9						
diff		25.0	44.0	79.4	65.5	49.9	3.5
rank		5.0	4.0	1.0	2.0	3.0	6.0
<i>1201</i>	37.3						
diff		97.7	110.8	110.0	77.3	58.5	9.8
rank		3.0	1.0	2.0	4.0	5.0	6.0
<i>1201a</i>	44.2						
diff		45.8	49.3	49.0	30.2	20.3	8.0
rank		3.0	1.0	2.0	4.0	5.0	6.0
<i>jansim</i>	81.0						
diff		43.7	42.5	58.5	41.8	32.4	20.4
rank		2.0	3.0	1.0	4.0	5.0	6.0
<i>augsim</i>	71.1						
diff		69.8	87.3	88.3	66.2	44.4	15.6
rank		3.0	2.0	1.0	4.0	5.0	6.0
Avg change		63.64	72.88	84.17	62.79	46.88	11.62
Avg rank		3.18	2.09	1.45	3.55	4.73	6.00
θ_v change ^a		0.059	0.070	0.041	0.034	0.029	na ^b

^a θ_v change estimated from moisture release curve data for corresponding avg. h change.^bNo moisture release curve data was measured at this depth to convert h to θ_v .

simulation (Fig. 3), the rainfall started at 18.458 d, and the wetting front reached 60 cm in 2.3 h, 90 cm in 2.8 h, 120 cm in 4.3 h, 160 cm in 5.3 h, and 200 cm in 8.5 h. In the SE pedon, rainfall started at 19.448 d, and the wetting front reached

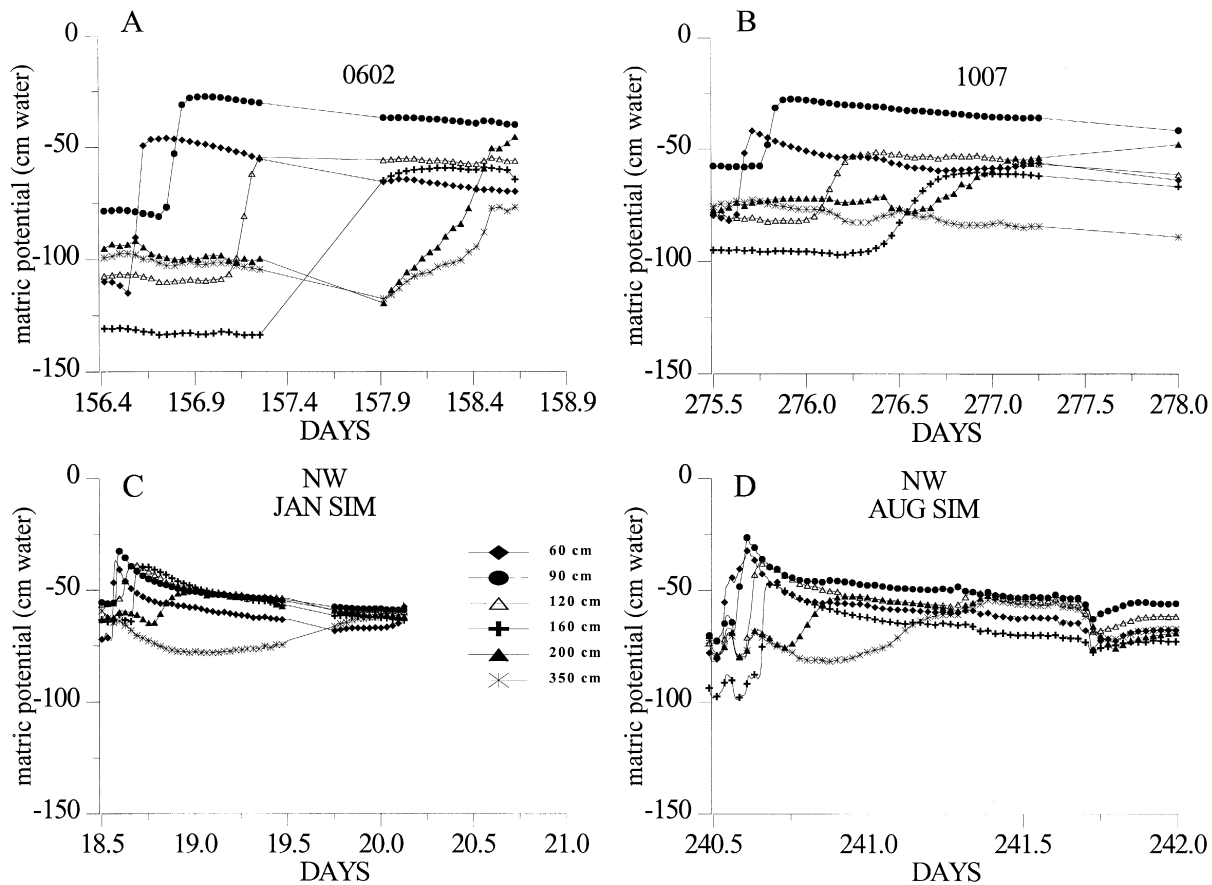


Fig. 3. Tensiometer data from the NW subplot for four events (0602, 1007, Jan. sim, and Aug. sim).

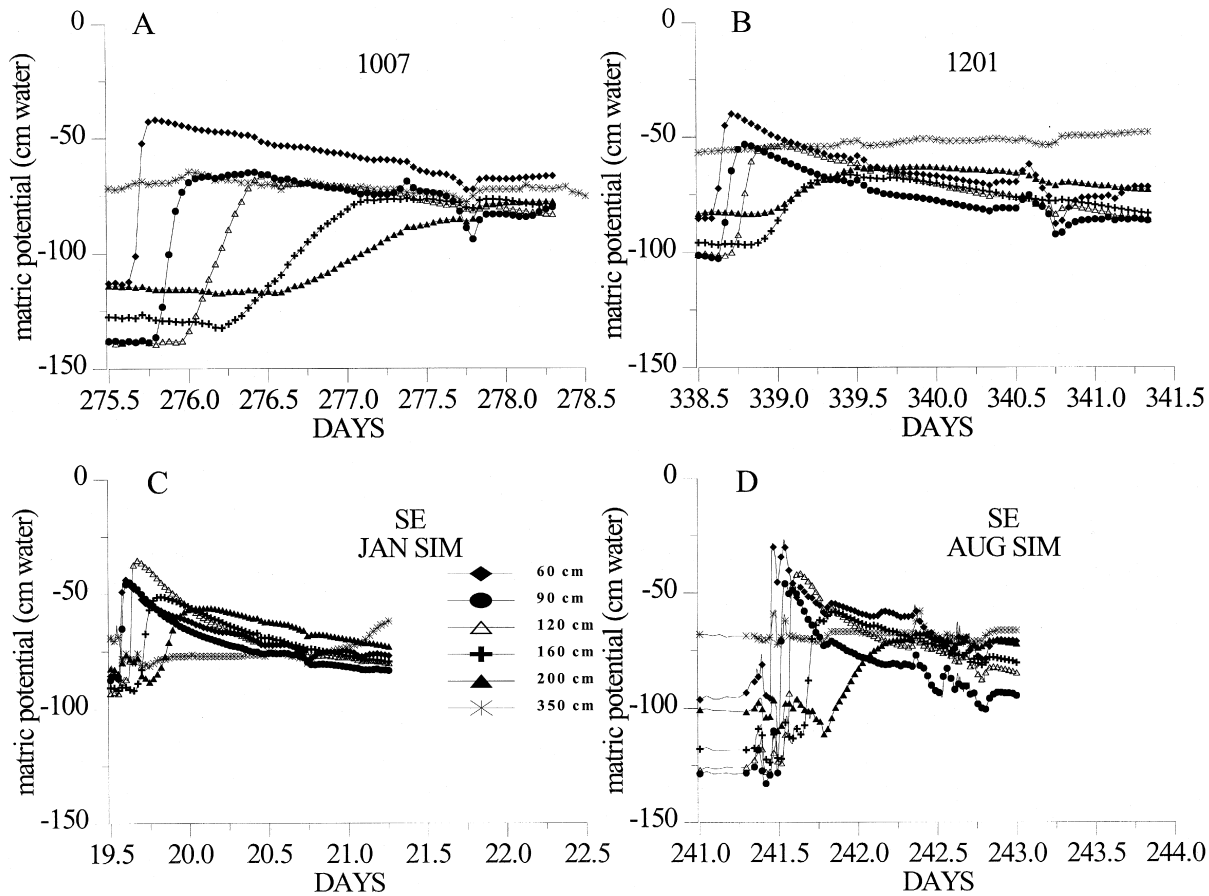


Fig. 4. Tensiometer data for the SE subplot for four events (1007, 1201, Jan. sim, and Aug. sim).

60 cm in 2.9 h, 90 cm in 3.3 h, 120 cm in 4.6 h, 160 cm in 6.5 h, and 200 cm in 9.8 h.

Depths with large differences between maximum and minimum potentials during rainfall events were hypothesized to be zones where vertical water movement slowed and subsequent lateral movement of water may occur (Tables 3 and 4). The greatest changes in potential (as per average rank) over all rainfall events were at 160 cm in the NW pedon (Table 3). This depth was within the Bt1 horizon, which had more clay, and a lower K_s than the rest of the profile. Although changes in potential were the largest in this Bt1 horizon, that does not indicate the highest changes in θ_v due to differences in water retention properties (Table 3). However, these data suggested there was some degree of decreased tensions associated with the upper part of this horizon. Potentials also changed appreciably in the NW pedon at 90 cm during the rainfall events (0602, 1007, Jan and Aug simulation; Fig. 3). Thus, there was an impedance to vertical movement that caused water to accumulate and the matric potential to increase at 90 cm in the NW pedon. These data suggested two zones of water accumulation during water percolation at the NW site, one in the E2 horizon (90 cm), and one in the Bt1 horizon (160 cm).

For the SE pedon, the 120 cm depth exhibited the greatest average change in matric potential. This was immediately above the horizon with the lowest K_s (Bt4 starts at 126 cm) (Table 4). These data suggested the Bt4 was impeding vertical flow and causing decreases in tension above this feature. This is similar to findings by Seyfried (1991) who found increases in moisture content above argillic horizons during infiltration events. However, significant differences in K_s between the SE Bt horizons were not evident (Table 1). Volumetric water content from January simulations indicated a zone of elevated θ_v at 60 cm in the SE pedon, and at 152 cm in the NW pedon during infiltration and redistribution (Fig. 5a and b). Elevated θ_v at 152 cm in the NW pedon was consistent with matric potential data, i.e., higher θ_v occurred at a depth where the largest changes in potential were noted.

Larger changes in matric potentials at the 350 cm depth occurred in the NW than in the SE subplot (avg. of 19 cm H_2O for NW, 11 cm H_2O for SE; Tables 3 and 4, and Figs. 3 and 4). Noticeable response of the 350 cm tensiometer occurred with most events in the NW pedon (0602, and Jan. and Aug. simulations) (Fig. 3), but was not as obvious in the SE pedon (1007, 1201a, Aug simulation) (Fig. 4). The SE pedon has a lower hydraulic conductivity overall, and higher water holding capacity, thus it is hypothesized it would take longer for wetting fronts to reach the 350 cm depth. Even over longer periods, there was typically very little change in matric potential at the 350 cm depth in the SE pedon (Fig. 4). Although water release curve data were not collected, the NW pedon at 350 cm was sandier than the SE pedon at 350 cm, thus a change in potential of 19 cm H_2O in the NW pedon represented a proportionally larger increase in θ_v than an 11 cm potential change in the SE pedon. These data

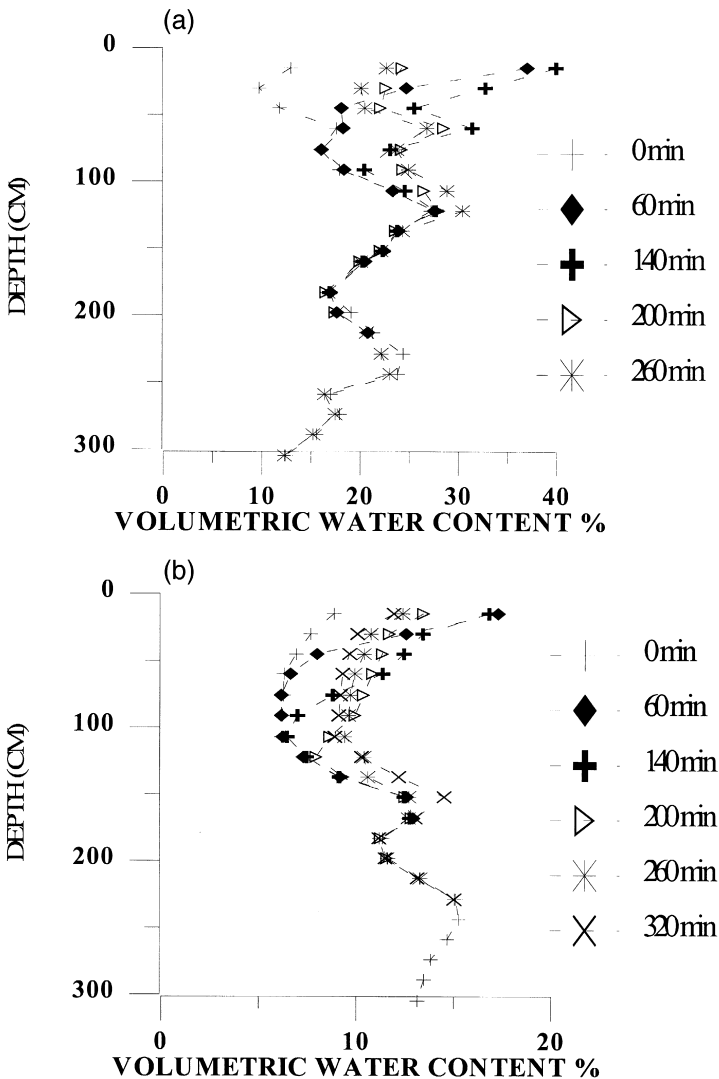


Fig. 5. Volumetric water content with depth for both subplots during the January simulation. (a) SE pedon; (b) NW pedon.

suggest larger quantities of water reached deeper portions of the profile in the NW pedon than in the SE pedon. This was interpreted to mean either more vertical water movement associated with the sandier pedon, more water retention in the subsoils of the loamier SE pedon, or differences in evapotranspiration (ET) between the pedons. Since ET in these subplots would be similar, data suggested less deep percolation (recharge) in the sites with loamier subsoils as compared to the sandier soils.

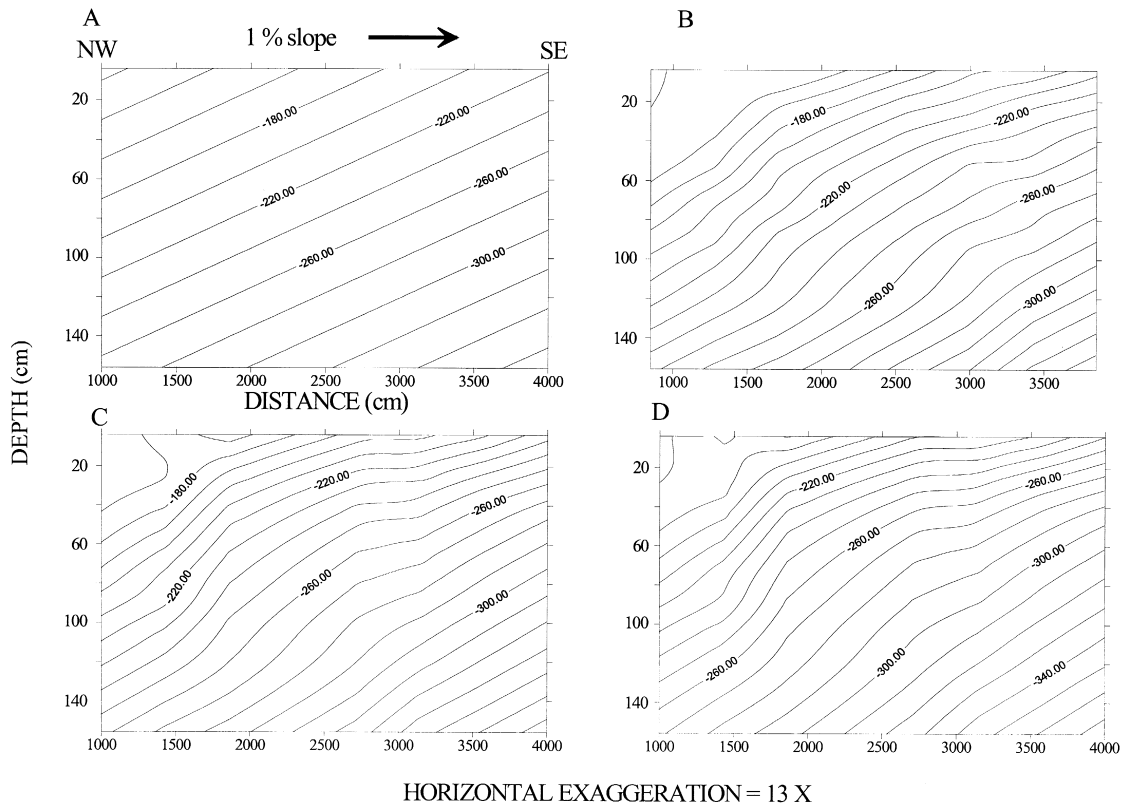


Fig. 6. VS2DT simulation model output (plots of total head — H) for a transect across a simulated landscape (1% slope) proceeding from NW to SE. (A) 0 h; (B) 20 h; (C) 40 h; (D) 70 h.

3.4. Modeling

The rationale for conducting simulation modeling for these data was to infer possible landscape dynamics of water movement. As discussed in the methods, VS2DT was used to simulate water flow on a slightly sloped (1%) landscape (Fig. 6). In conducting these simulations, it was fully evident that slope dictates a major portion of the initial (time 0) lateral gradients. We used a 1% slope because it typified our site. Initial conditions (time 0) are shown in Fig. 6A.

At the 20 h time step (Fig. 6B), an enhanced gradient was predicted to occur leading into the Bt horizon of the middle (NE-type) soil. This gradient became better expressed at the 40 h (Fig. 6C) and 70 h (Fig. 6D) time step. This is hypothesized to be due to a retarded wetting front resulting in deeper horizons (within and below the argillic horizon) remaining dry why the encroaching lateral front wets to deeper depths in adjacent soils. Concurrently, because the wetting front moves slightly quicker in the sandy NW soil, the gradients into the subjacent drier subsoil develops. Thus, enhanced gradients developed leading into these relatively drier zones on the landscape, and local effects of soil types are evident.

Across the landscape through all time periods, fairly steep lateral flow gradients were predicted above 2 m, although correlating this to any particular soil feature (such as the top of the argillic horizon) was difficult. However, these simulations did indicate that the solum is predicted to have large effects on landscape water movement, even though the separate effects of contrasting horizons were not readily observable.

3.5. Tracer studies

Analysis of tracer movement during the August rainfall simulation events was evaluated by examining sampling depths and locations where Br was detected. Our soil sampling measured the resident concentration of Br that existed at the specified time and depth. Although we measured resident concentrations and we were particularly interested in Br fluxes, as a relative assessment higher resident concentrations indicated areas where Br had migrated.

A few unsystematic, elevated tracer concentrations were detected in both the SE and NW pedons. This was attributed to either macropore presence, or possible contamination/error during sampling and analyses. Although macropore transport is an important aspect of solute movement, it was not the focus of this study. In addition, Ghodrati and Jury (1990) displayed some of the potential problems associated with core sampling during tracer or dye studies. Basically, local vertical and horizontal variability can be extreme. For this reason, only elevated Br concentrations that had adjacent (either in spatial — x , y , z or temporal dimensions) elevated concentrations were interpreted to be evidence of

directional tracer movement. These results could still be impacted by preferential flowpaths, but we felt with our approach, this would be limited.

Bromide movement in the NW pedon showed that at 45 h, the Br had reached the 200 cm depth in the plot center (60 mg kg⁻¹) (Fig. 7). In this profile, there was little lateral tracer movement. However, at 65 cm east from the center at the 11-h sampling time at the 160 and 200 cm depths, very small amounts of Br were detected. These depths were within the argillic horizon (Bt1 and Bt2, respectively) of this NW pedon. Minor Br presence laterally from the center indicated a slight eastward lateral movement associated with the NW argillic horizon. This zone had large differences in matric potentials during rainfall events, and possessed marginally lower *K_s*. These tracer analyses support minor lateral movement within the argillic horizon of this pedon. However, because observations of elevated Br concentrations laterally from the center were only detected at one sampling period, these data suggested limited movement.

In the SE plot, Br migrated to the 160-cm depth in the center after 45 h (Fig. 8), but concentrations were lower (6 mg kg⁻¹) than in the NW pedon, suggesting tracer was being retarded (physically and/or chemically) in this pedon. There was a slight lateral solute migration in the 1-h sampling period in the north (detected at 65 and 90 cm from the center) and south directions (detected at 40 cm from center), at depths of 15 and 30 cm. Lateral Br movement in two directions in the 1st hour of sampling may indicate pulse spreading, and not unidirectional movement. This could be associated with vertical flow

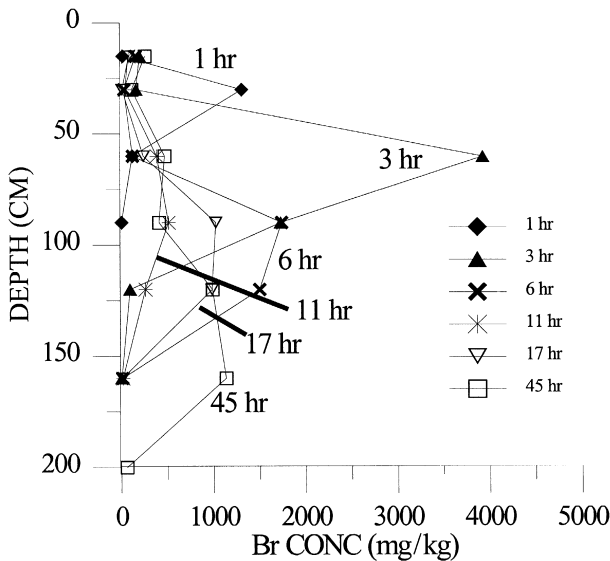


Fig. 7. Br⁻ concentrations in the soils at the center of the application plot during the August simulation for the NW pedon.

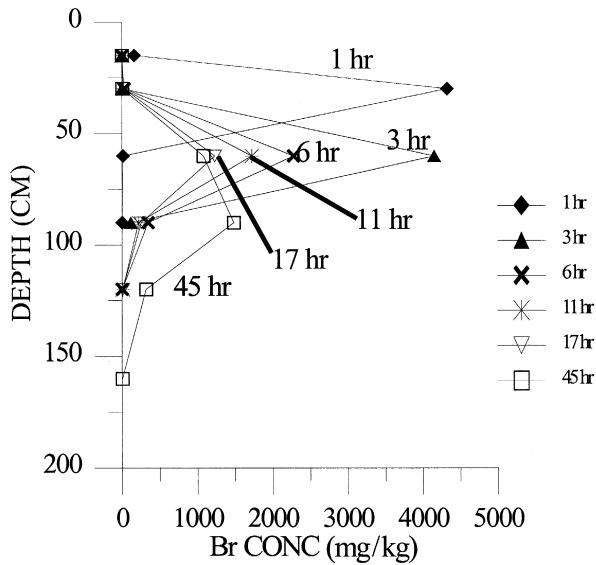


Fig. 8. Br⁻ concentrations in the soils at the center of the application plot during the August simulation for the SE pedon.

impedance caused by a traffic or plow pan. Similarly, Reuter et al. (1998) found lateral flow on a loess-derived hillslope was associated with Ap and Bw horizons, which was shallower in the profile than originally hypothesized. After the pulse had passed in the center during later times, no Br was detected laterally in these upper portions. In later time steps, Br was also detected laterally to the south at the 60 (Bt2) and 90 (Bt3) cm depths after 17 (60 and 90 cm) and 45 h (90 cm). Amounts detected were small compared to the center pulse; < 1.0% of the pulse was detected laterally. Thus, it is evident that only slight evidence of lateral migration of tracer was observed with these tracer analyses.

It was unclear why some of the slight lateral migration observed occurred in upper portions of the argillic horizon in the SE pedon. Certainly, preferential flowpaths could result in these observations. Another hypothesis might be that under unsaturated conditions, horizons that had higher K_s with respect to other horizons dominantly had lower calculated $K(h)$ with respect to the rest of the profile. In this instance, the calculated $K(h)$ for the Bt3 horizon was low as compared to the above and below horizons (Fig. 9). For example, at 17 h after rainfall application, the Bt2 matric potential (60 cm) was -60.5 cm H₂O, and was -79.6 cm H₂O for the Bt2/Bt3 interface (90 cm). The $K(h)$ at these matric potentials would be 3.6×10^{-4} cm h⁻¹ for the Bt2, and 9.9×10^{-6} cm h⁻¹ for the Bt2/Bt3 interface (using Bt3 data). Similarly, matric potentials at 60 cm (-70.6 cm H₂O) and 90 cm (-93.3 cm H₂O) at 45 h showed similar

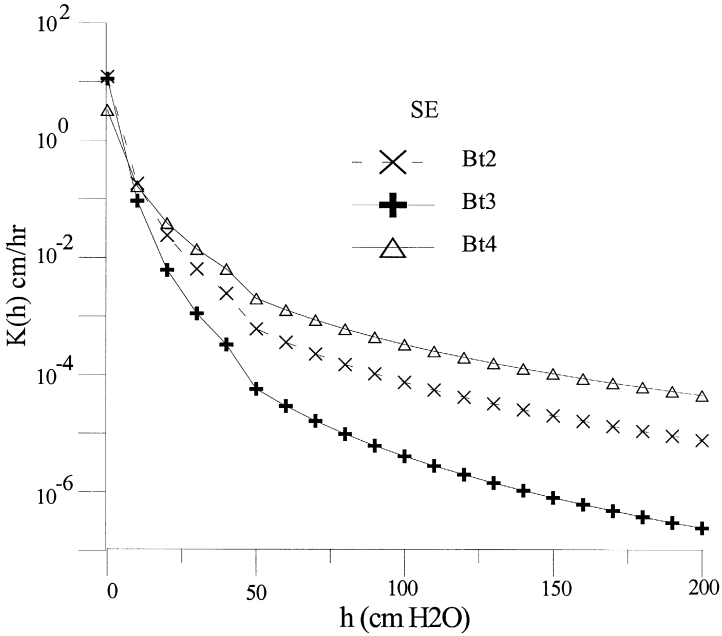


Fig. 9. $K(h)$ (log scale) curves for the Bt2, Bt3, and Bt4 horizons from the SE pedon.

differences in $K(h)$. It is hypothesized that under unsaturated conditions, the Bt3 horizon was acting as a hydraulic impedance. It is possible that analyses at longer sampling times might have displayed lateral tracer movement at greater depths in the SE pedon. Bromide concentrations in the center (120 and 160 cm depth) at these times (17 and 45 h) were low (0.6 to 317.0 mg kg⁻¹), thus any lateral movement of Br may have been below detection limits.

4. Conclusions

It is hypothesized that the reason for the relatively large effect of particle size on hydraulic properties was due to the lack of well-developed soil structure, especially in upper horizons. Soil descriptions and breakthrough curves (Shaw et al., 2000) indicated a lack of well-developed structure in the upper portions of both profiles, with increasing structure development with depth.

Maximum changes in matric potentials associated with wetting fronts, interpreted to indicate possible locations of perched water in these profiles, were mainly associated with horizons of lower K_s (120 cm depth in the SE pedon, 160-cm depth in the NW pedon), even when K_s differences were not significant. A very slight lateral tracer movement in the NW pedon occurred at the

160-cm depth (Bt1 horizon), and coincided with depths where changes in matric potentials were maximal and K_s were lower. Minor amounts of lateral movement of tracer were detected at 60 and 90 cm in the SE pedon. Unlike the NW pedon, these depths do not correspond to maximal matric potential changes nor minimal K_s . It was not completely clear why lateral migration of tracer was observed at these depths. As mentioned above, because of the minor amounts observed preferential flow could impact observations. Alternatively, $K(h)$ at tensions typical during redistribution events were lower in the Bt3 than the Bt2, so differences in $K(h)$ might induce slight lateral flow. Data suggested the degree of flow impedance and lateral movement was slightly different between NW and SE soils. Monitoring of matric potentials suggested less deep percolation (> 3.5 m) occurred in the loamier SE soils than the sandier NW soils.

In this study, lateral movement of Br was small. We did observe evidence from changes in matric potentials that horizons of low K_s were acting as impeding layers, and it was apparent that lateral flow would ensue if gradients existed. Hydrologic modeling indicated lateral gradients of flow associated with the solum could occur on these landscapes. These and similar data could be used to develop more efficient irrigation strategies as well as predict areas more susceptible to accelerated groundwater contamination due to enhanced leaching.

References

- Amoozegar, A., 1989. A compact constant-head permeameter for measuring saturated hydraulic conductivity of the vadose zone. *Soil Sci. Soc. Am. J.* 53, 1356–1361.
- Anderson, M.G., Burt, T.P., 1990. Subsurface runoff. *Process Studies of Hillslope Hydrology*. Wiley, New York, pp. 365–400.
- Blake, R., Hartge, K.H., 1986. Bulk density. In: Klute, A. (Ed.), *Methods of Soil Analysis, Part 1: Physical and Mineralogical Methods*, 2nd edn. Agron. Monogr. 9. ASA and SSSA, Madison, WI.
- Blume, L.J., Perkins, H.F., Hubbard, R.K., 1987. Subsurface water movement in an upland Coastal Plain soil as influenced by plinthite. *Soil Sci. Soc. Am. J.* 51, 774–779.
- Bosch, D.D., West, L.T., 1998. Hydraulic conductivity variability for two sandy soils. *Soil Sci. Soc. Am. J.* 62, 90–98.
- Bosch, D.D., Hubbard, R.K., West, L.T., Lowrance, R.R., 1994. Subsurface flow patterns in a riparian buffer system. *Trans. ASAE* 37, 1783–1790.
- Bruce, R.R., Whisler, F.D., 1973. Infiltration of water into layered field soils. *Ecological Studies for Physics of Soil Water and Salts*. pp. 78–89.
- Butters, G.L., Cardon, G.E., 1998. Temperature effects on air-pocket tensiometers. *Soil Sci.* 163, 677–685.
- Cassel, D.K., Klute, A., 1986. Water potential: tensiometry. In: Klute, A. (Ed.), *Methods of Soil Analysis, Part 1: Physical and Mineralogical Methods*, 2nd edn. Agron. Monogr. 9. ASA and SSSA, Madison, WI.
- Chappall, N.A., Ternan, J.L., Williams, A.G., Reynolds, B., 1990. Preliminary analysis of water and solute movement beneath a coniferous hillslope in Mid-Wales, UK. *J. Hydrol.* 116, 201–215.

- Gaskin, J.W., Dowd, J.F., Nutter, W.L., Swank, W.T., 1989. Vertical and lateral components of soil nutrient flux in a hillslope. *J. Environ. Qual.* 18, 403–410.
- Ghodrati, M., Jury, W.A., 1990. A field study using dyes to characterize preferential flow of water. *Soil Sci. Soc. Am. J.* 54, 1558–1563.
- Hicks, D.W., McConnell, J.B., Hubbard, R.K., 1991a. Effect of the unsaturated zone on the migration and retardation of a conservative tracer at the Plains, Georgia Research site. In: US Geological Survey, Water-Resources Investigations Report 91-88.
- Hicks, D.W., McConnell, J.B., Asmussen, L.E., Leonard, R.A., Smith, C.N., 1991b. Movement and fate of agricultural chemicals in the surface and subsurface environments near Plains, Southwestern Georgia-Integrated Work Plan. US Geological Survey, Open-File Report 91-73.
- Jury, W.A., Gardner, W.R., Gardner, W.H., 1991. *Soil Physics*. Wiley, 328 pp.
- Katul, R., Todd, G.P., Pataki, D., 1997. Soil water depletion by oak trees and the influence of root water uptake on the moisture content spatial statistics. *Water Resour. Res.* 33, 611–623.
- Kilmer, V.J., Alexander, L.T., 1949. Methods of making mechanical analysis of soils. *Soil Sci.* 68, 15–24.
- Klute, A., Dirksen, C., 1986. Hydraulic conductivity and diffusivity: laboratory methods. In: Klute, A. (Ed.), *Methods of Soil Analysis, Part 1: Physical and Mineralogical Methods*, 2nd edn. Agron. Monogr. 9. ASA and SSSA, Madison, WI.
- Kung, K.J., 1990a. Preferential flow in a sandy vadose zone: 1. Field observation. *Geoderma* 46, 51–58.
- Kung, K.J., 1990b. Preferential flow in a sandy vadose zone: 2. Mechanism and implications. *Geoderma* 46, 59–71.
- Lappala, E.G., Healy, R.W., Weeks, E.P., 1993. Documentation of computer program VS2DT to solve the equations of fluid flow in variably saturated porous media. USGS Report 83-4099, Denver, CO.
- Leonard, R.A., Marti, L.R., Hicks, D.W., McConnell, J.B., 1993. Fate and transport of Atrazine at the Plains, Georgia, Ground Water Study Site, unpublished.
- McDonnell, J.J., 1990. A rationale for old water discharge through macropores in a steep, humid catchment. *Water Resour. Res.* 26, 2821–2832.
- Nyberg, L., 1995. Water flow path interactions with soil hydraulic properties in till soil at Gardsjon, Sweden. *J. Hydrol.* 170, 255–275.
- Pilkinton, J.A., 1974. *Soil Survey of Schley and Sumter Counties, Georgia*. United States Department of Agriculture in cooperation with the University of Georgia, Agricultural Experiment Station.
- Reuter, R.J., McDaniel, P.A., Hammel, J.E., Falen, A.L., 1998. Solute transport in seasonal perched water tables in loess-derived soils. *Soil Sci. Soc. Am. J.* 62, 977–983.
- Ross, D.S., Bartlett, R.J., Magdoff, F.R., Walsh, G.J., 1994. Flow path studies in forested watersheds of headwater tributaries of Brush Brook, Vermont. *Water Resour. Res.* 30, 2611–2618.
- Seyfried, M.S., 1991. Infiltration patterns from simulated rainfall on a semiarid rangeland soil. *Soil Sci. Soc. Am. J.* 55, 1726–1734.
- Shaw, J.N., West, L.T., Radcliffe, D.E., Bosch, D.D., 2000. Preferential flow and pedotransfer functions for transport properties in sandy Kandicudults. *Soil Sci. Soc. Am. J.*, in press.
- Shaw, J.N., West, L.T., Truman, C.C., Radcliffe, D.R., 1997. Morphologic and hydraulic properties of soils with water restrictive horizons in the Georgia Coastal Plain. *Soil Sci.* 162, 875–885.
- Soil Survey Staff, 1996. *National Soil Survey Handbook*. USDA-Natural Resources Conservation Service, National Soil Survey Center, Lincoln, NE.
- Stewart, L.M., Hicks, D.W., 1996. Hydrogeology of the interstream area between Ty Ty Creek and Ty Ty Creek tributary near Plains, Georgia. US Geological Survey Water-Resources Investigations Report 96-4052.

- van Genuchten, M.T., 1980. A closed form equation for predicting the hydraulic conductivity of unsaturated soil. *Soil Sci. Soc. Am. J.* 44, 89–898.
- Wilson, G.V., Jardine, P.M., O'Dell, J.D., Collineau, M., 1993. Field-scale transport from a buried line source in variably saturated soil. *J. Hydrol.* 145, 83–109.
- Wilson, G.V., Jardine, P.M., Luxmoore, R.J., Zelazny, L.W., Lietzke, D.A., Todd, D.E., 1991. Hydrogeochemical processes controlling subsurface transport from an upper subcatchment of Walker Branch watershed during storm events: 1. Hydrologic transport processes. *J. Hydrol.* 123, 297–316.
- Wilson, G.V., Jardine, P.M., Luxmoore, R.J., Jones, J.R., 1990. Hydrology of a forested hillslope during storm events. *Geoderma* 46, 119–138.